

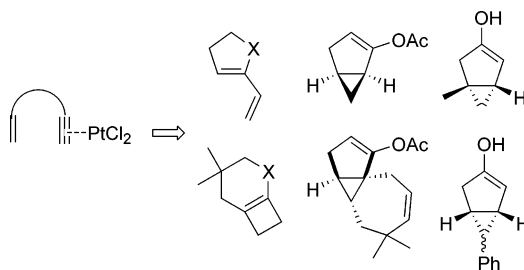
Theoretical Analysis of the High Versatility in PtCl₂-Mediated Cycloisomerization of Enynes on a Common Mechanistic Basis

Elena Soriano^{*,†} and José Marco-Contelles[‡]

Laboratorio de Resonancia Magnética, Instituto de Investigaciones Biomédicas (CSIC), C/Arturo Duperier 4, 28029-Madrid, Spain, and Laboratorio de Radicales Libres, IQOG (CSIC), C/Juan de la Cierva 3, 28006-Madrid, Spain

esoriano@arrakis.es

Received July 11, 2005

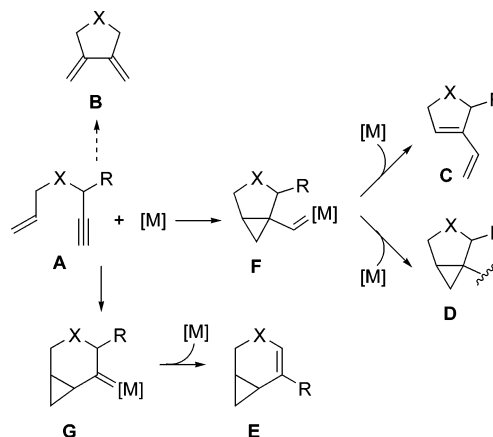


Transformations of enynes upon treatment with electrophilic transition-metal complexes, such as PtCl₂, are strongly substrate-dependent processes and may yield a wide variety of cyclic compounds. Despite the high versatility, many of these processes could be closely related from a mechanistic point of view. Theoretical analyses of the plausible reaction mechanisms provide support for a unified mechanistic picture based on the electrophilic activation of the triple bond by the catalyst, which triggers the nucleophilic alkene attack through an endo- or exo-cyclization mode, to form the cyclopropylcarbene species. Then, these common key intermediates may evolve through alternative paths to afford a range of cyclic compounds. The preference for each path and the evolution of these intermediates are governed by the nature of the starting enyne. The effects induced by different structural motifs, such as the role played by a heteroatom directly attached to the triple bond, the tether length, the substitution on the acetylenic position, and the *gem*-dialkyl substitution on the tether, among others, are discussed. The proposed common mechanistic scheme can rationalize and account for the experimental observations accumulated.

Introduction

The high synthetic potential of polyunsaturated systems such as enynes has made possible the preparation of a wide variety of carbo- and heterocyclic building blocks via transition-metal-catalyzed reactions.¹ These processes depend not only on the catalyst system but strongly on the structure of the precursor **A** and, accordingly, may yield different kind of products: Alder-ene adduct **B**,^{2,3} metathesis product **C**,⁴ and diverse cyclopropyl derivatives **D** and **E** (Scheme 1).^{5–7} Remarkably, minor changes of the reaction conditions and/or substrate structures can lead to different products. Moreover, most of these transformations take place under regio- and stereochem-

SCHEME 1



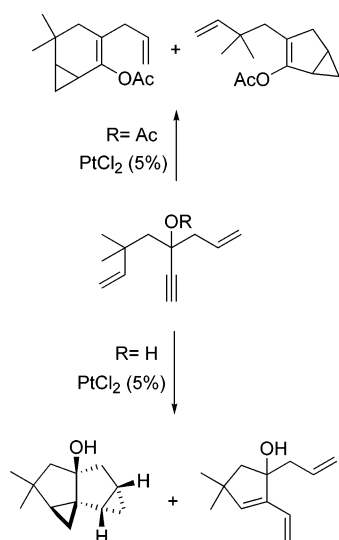
ical control. One fascinating extension of this chemistry to dienynes has shown that the nature of an oxygenated functionality at the propargylic position critically controls

[†] Instituto de Investigaciones Biomédicas (CSIC).

[‡] IQOG (CSIC).

(1) (a) Lloyd-Jones, G. C. *Org. Biomol. Chem.* **2003**, *1*, 215–236. (b) Méndez, M.; Mamane, V.; Fürstner, A. *Chemtracts* **2003**, *16*, 397–425. (c) Aubert, C.; Buisine, O.; Malacria, M. *Chem. Rev.* **2002**, *102*, 813–834.

SCHEME 2



the regio- and stereochemistry of the PtCl₂-mediated cycloisomerization reaction.⁸ Thus, upon treatment with PtCl₂, tertiary propargylic alcohols (or ethers) that bear two unsaturated chains at the propargylic position yield tetracyclic compounds, while analogous propargylic esters provide completely different products, bicyclic enol esters (Scheme 2).

This high versatility, though synthetically attractive, needs a deep mechanistic understanding to direct the catalyzed cycloisomerization to the desired product. As a part of an extensive study of PtCl₂-mediated cycloisomerizations of diverse polyunsaturated systems,^{9,10} we present herein additional mechanistic insights on the basis of theoretical DFT analysis. Our previous studies on the cycloisomerization of enynes have pointed to a common mechanistic basis, which may diverge to such different cycloisomerizations.^{9,10b} The activation of the triple bond by electrophilic metal complexes, such as

platinum, palladium, ruthenium, and gold complexes or salts, among others, generates highly electrophilic species and triggers the nucleophilic addition of the double bond to yield metal–cyclopropylcarbene¹¹ intermediates **F** and **G** (Scheme 1) through an exo- or endo-pathway. Regarding these key species, they could be also envisaged as cyclopropyl carbinyl cations¹² stabilized by the metal complex, in line with the cationic manifold suggested by Fürstner.⁶ The degree of metal–carbenic vs metal-stabilized carbocation character may rely on the catalyst system¹³ and reaction conditions.

We now report new studies on PtCl₂-mediated transformations of enynes. Whereas our previous works have analyzed the role of the propargylic substituents in the cycloisomerization of 1,6-enynes,^{9,10b} the current report is devoted to the study of the effects arising from the substitution and tether length. First, we focus on the cycloisomerization of 1,6- and 1,7-ene-ynamides and on the role played by the nitrogen atom directly attached to the triple bond. Next, we analyze the cycloisomerization of en-1-yn-3-ol systems and the role of the tether length, substitution on the terminal alkyne carbon, and the *gem*-dialkyl substitution on the tether.

Computational Methods

Calculations have been carried out using Gaussian03.¹⁴ The geometries have been fully optimized at the DFT level by means of the B3LYP hybrid functional.¹⁵ In the last years, the satisfactory performance for this method in the chemistry of transition metals has been frequently reported.¹⁶ To check the reliability of B3LYP for these transition-metal systems, a comparison between B3LYP and MP2 methods for a reduced model has been performed, and the results justify the choice.¹⁷ The standard 6-31G(d) basis set has been applied for all the atoms except Pt. Pt atom has been described by the LANL2DZ basis set,¹⁸ where the innermost electrons are replaced by a relativistic ECP and the 18 valence electrons are explicitly treated by a double- ζ basis set.

(10) (a) Soriano, E.; Marco-Contelles, J. *Chem. Eur. J.* **2005**, *11*, 521–533; (b) Soriano, E.; Ballesteros, P.; Marco-Contelles, J. *J. Org. Chem.* **2004**, *69*, 8018–8023.

(11) (a) Bruneau, C. *Angew. Chem., Int. Ed.* **2005**, *44*, 2328–2334. (b) Echavarren, A. M.; Nevado, C. *Chem. Soc. Rev.* **2004**, *33*, 431–436.

(12) Wiberg, K. B.; Shobe, D.; Nelson, G. L. *J. Am. Chem. Soc.* **1993**, *115*, 10645–10652.

(13) Nieto-Oberhuber, C.; Muñoz, M. P.; Buñuel, E.; Nevado, C.; Cárdenas, D. J.; Echavarren, A. M. *Angew. Chem., Int. Ed.* **2004**, *43*, 2402–2406.

(14) Frisch, M. J.; Trucks, G. W.; Schlegel, H. B.; Scuseria, G. E.; Robb, M. A.; Cheeseman, Montgomery, J. A.; Vreven, T.; Kudin, K. N.; Burant, J. C.; Millam, J. M.; Iyengar, S. S.; Tomasi, J.; Barone, V.; Mennucci, B.; Cossi, M.; Scalmani, G.; Rega, N.; Petersson, G. A.; Nakatsuji, H.; Hada, M.; Ehara, M.; Toyota, K.; Fukuda, R.; Hasegawa, J.; Ishida, M.; Nakajima, T.; Honda, Y.; Kitao, O.; Nakai, H.; Klene, M.; Li, X.; Knox, J. E.; Hratchian, H. P.; Cross, J. B.; Adamo, C.; Jaramillo, J.; Gomperts, R.; Stratmann, R. E.; Yazyev, O.; Austin, A. J.; Cammi, R.; Pomelli, C.; Ochterski, J. W.; Ayala, P. Y.; Morokuma, K.; Voth, G. A.; Salvador, P.; Dannenberg, J. J.; Zakrzewski, V. G.; Dapprich, S.; Daniels, A. D.; Strain, M. C.; Farkas, O.; Malick, D. K.; Rabuck, A. D.; Raghavachari, K.; Foresman, J. B.; Ortiz, J. V.; Cui, Q.; Baboul, A. G.; Clifford, S.; Cioslowski, J.; Stefanov, B. B.; Liu, G.; Liashenko, A.; Piskorz, P.; Komaromi, L.; Martin, R. L.; Fox, D. J.; Keith, T.; Al-Laham, M. A.; Peng, C. Y.; Nanayakkara, A.; Challacombe, M. P.; Gill, M. W.; Johnson, B. G.; Chen, W.; Wong, M. W.; González, C.; Pople, J. A. *Gaussian 03*, Revision B.03; Gaussian, Inc.: Pittsburgh, PA, 2003.

(15) (a) Lee, C.; Yang, W.; Parr, R. *Phys. Rev. B* **1988**, *37*, 785–789. (b) Becke, A. J. *Chem. Phys.* **1993**, *98*, 5648–5652.

(16) (a) Koch, W.; Holthausen, M. C. *A Chemist's Guide to Density Functional Theory*, Wiley-VCH: Weinheim, **2000**; (b) Niu, S.; Hall, M. B. *Chem. Rev.* **2000**, *100*, 353–406.

(17) See the Supporting Information for details.

(18) Hay, P. J.; Wadt, W. R. *J. Chem. Phys.* **1985**, *82*, 270–283.

(2) Some examples for carbocyclic compounds: (a) Trost, B. M.; M. J. Krische, M. J. *Synlett* **1998**, 1–16. (b) Trost, B. M.; Lautens, M.; Chan, C.; Jebaratnam, D. J.; Mueller, T. *J. Am. Chem. Soc.* **1991**, *113*, 636–644. (c) Trost, B. M.; Krische, M. J. *J. Am. Chem. Soc.* **1999**, *121*, 6131–6141. (d) Trost, B. M.; Corte, J. R.; Gudiksen, M. S. *Angew. Chem., Int. Ed. Engl.* **1999**, *38*, 3662–3664. (e) Takayama, Y.; Okamoto, S.; Sato, F. *J. Am. Chem. Soc.* **1999**, *121*, 3559–3560. (f) Trost, B. M.; Haffner, C. D.; Jebaratnam, D. J.; Krische, M. J.; Thomas, A. P. *J. Am. Chem. Soc.* **1999**, *121*, 6183–6192. (g) B. M. Trost, B. M.; Toste, F. D. *J. Am. Chem. Soc.* **2000**, *122*, 714–715.

(3) Formation of heterocyclic compounds: (a) Trost, B. M.; Pedregal, C. *J. Am. Chem. Soc.* **1992**, *114*, 7292–7294. (b) Goeke, A.; Sawamura, M.; Kuwano, R.; Ito, Y. *Angew. Chem., Int. Ed. Engl.* **1996**, *35*, 662–663. (c) Lei, A.; Waldkirch, J. P.; He, M.; Zhang, X. *Angew. Chem., Int. Ed.* **2002**, *41*, 4526–4529.

(4) (a) Diver, S. T.; Giessent, A. *J. Chem. Rev.* **2004**, *104*, 1317–1382. (b) Mori, M. *Topics in Organometallic Chemistry*; Fürstner, A., Ed.; Springer-Verlag: Berlin, 1998; Vol. 1, p 133–154. (c) Fürstner, A. *Angew. Chem., Int. Ed.* **2000**, *39*, 3012–3043. (d) Poulsen, C. S.; Madsen, R. *Synthesis* **2003**, 1–18.

(5) Blum, J.; Beerkräft, H.; Badrieh, Y. *J. Org. Chem.* **1995**, *60*, 5567–5569.

(6) (a) Fürstner, A.; Szillat, H.; Stelzer, F. *J. Am. Chem. Soc.* **2000**, *122*, 6785–6786. (b) Fürstner, A.; Stelzer, F.; Szillat, H. *J. Am. Chem. Soc.* **2001**, *123*, 11863–11869.

(7) Méndez, M.; Muñoz, M. P.; Nevado, C.; Cárdenas, D. J.; Echavarren, A. M. *J. Am. Chem. Soc.* **2001**, *123*, 10511–10520.

(8) Mainetti, E.; Mouries, V.; Fensterbank, L.; Malacria, M.; Marco-Contelles, J. *Angew. Chem., Int. Ed.* **2002**, *41*, 2132–2135.

(9) (a) Soriano, E.; Ballesteros, P.; Marco-Contelles, J. *Organometallics* **2005**, *24*, 3172–3181. (b) Soriano, E.; Ballesteros, P.; Marco-Contelles, J. *Organometallics* **2005**, *24*, 3182–3191.

TABLE 1. Total^a and Free^b Energy Differences Computed for PtCl₂-Mediated Cycloisomerization of Ene-Ynamides

<i>n</i> = 1	ΔE (kcal mol ⁻¹)	ΔG_{298} (kcal mol ⁻¹)	<i>n</i> = 2	ΔE (kcal mol ⁻¹)	ΔG_{298} (kcal mol ⁻¹)
1	0.00	0.00	4	0.00	0.00
TS1	+7.60	+11.39	TS1	+7.87 (+6.62) ^c	+11.10 (+9.76) ^c
2	-9.74	-7.15	5	-13.21 (-11.84) ^c	-9.44 (-8.86) ^c
TS2	+5.68	+9.10	TS2	+4.82	+9.36
3	-16.89	-13.12	6	-20.63	-16.67

^a Zero-point corrected values. ^b Includes thermal corrections at 298 K. ^c Values for the first step of the cycloisomerization of the ene-ynamide bearing a *gem*-dimethyl substitution on the tether are given in parentheses.

TABLE 2. Comparison between Total^a and Free^b Energy Differences for the Electrocyclic Ring Opening of the Cyclobutene Intermediate vs Isomerization of the Exo-Double Bond for Ene-Ynamides^c

<i>n</i> = 1	ΔE (kcal mol ⁻¹)	ΔG_{298} (kcal mol ⁻¹)	<i>n</i> = 2	ΔE (kcal mol ⁻¹)	ΔG_{298} (kcal mol ⁻¹)
7	0.00	0.00	8	0.00	0.00
TS3	+25.86	+23.46	TS3	+32.88 (+31.97)	+32.64 (+31.01)
9	-18.64	-21.25	10	-11.78 (-11.01)	-10.77 (-10.56)
11	+1.45	+1.23	12	-4.91 (-5.15)	-5.02 (-6.05)

^a Zero-point corrected values. ^b Includes thermal corrections at 298 K. ^c Values for the ene-ynamide bearing a *gem*-dimethyl substitution on the tether (*n* = 2) are given in parentheses.

Harmonic frequencies were calculated at the optimization level, and the nature of the stationary points was determined according to the right number of negative eigenvalues of the Hessian matrix. The intrinsic reaction coordinate (IRC) pathways^{19a} from the transition structures have been followed using a second-order integration method,^{19b} to verify the expected connections of the first-order saddle points with the correct local minima found on the potential energy surface. Zero-point vibration energy (ZPVE) and thermal corrections (at 298 K) to the energy have been estimated on the basis of the frequency calculations at the optimization level and scaled by the recommended factor.

Natural bond orbital (NBO) analysis²⁰ has been performed by the module NBO v.3.1 implemented in Gaussian03 to evaluate the NPA atomic charges and delocalization interactions.

The structures summarized in Table 3 were optimized in aqueous solution ($\epsilon = 78.4$) at the B3LYP/6-31G(d)/CPCM level, where the solvent effects were evaluated by using the Gaussian03 implementation of the CPCM model,²¹ which employs conductor rather than dielectric boundary conditions.²² For this work, the default choices of the program for the recommended standard CPCM parameters were selected.

Results and Discussion

1. PtCl₂-Mediated Cycloisomerization of Ene-Ynamides. The transition-metal-catalyzed synthesis of heterocycles from enyne derivatives has become an efficient and selective synthetic protocol.²³ In this context,

(19) (a) Fukui, K. *Acc. Chem. Res.* **1981**, *14*, 363–368. (b) González, C.; Schlegel, H. B. *J. Phys. Chem.* **1990**, *94*, 5523–5527.

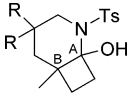
(20) (a) Reed, A. E.; Weinhold, F. *J. Chem. Phys.* **1983**, *78*, 4066–4073. (b) Reed, A. E.; Curtiss, L. A.; Weinhold, F. *Chem. Rev.* **1988**, *88*, 899–926.

(21) (a) Barone, V.; Cossi, M. *J. Phys. Chem. A* **1998**, *102*, 1995–2001. (b) Cossi, M.; Rega, N.; Scalmani, G.; Barone, V. *J. Comput. Chem.* **2003**, *24*, 669–681.

(22) Klamt, A.; Schüürmann, G. *J. Chem. Soc., Perkin Trans 2* **1993**, 799–805.

(23) For synthesis of heterocycles from enyne-derivatives catalyzed by related Pd(II) complexes: (a) Wolfe, J. P.; Thomas, J. S. *Curr. Org. Chem.* **2005**, *9*, 625–655. (b) Kirsch, G.; Hesse, S.; Comel, A. *Curr. Org. Synth.* **2004**, *1*, 47–63.

TABLE 3. Relative Free Energies in Aqueous Solution^a (kcal mol⁻¹) for the Syn/Anti Stereoselectivity in the Hydrolysis Reaction^a (For comparison of the thermodynamic stability, values are relative to the cyclobutanone form)

	chirality (A,B) ^b	R = H	chirality (A,B) ^b	R = CH ₃
		trans	<i>S,R</i>	+17.88
trans	<i>R,S</i>	+21.89	<i>R,R</i>	+17.26
cis	<i>S,S</i>	+11.93	<i>S,R</i>	-2.38
cis	<i>R,R</i>	+6.89	<i>R,S</i>	+0.65
cyclobutanone		0.00		0.00

^a Optimized geometries in aqueous solution at the B3LYP/6-31G(d)/CPCM level. ^b Chirality referred to “A” and “B” bridgehead positions, respectively. We have assumed a chair-type conformation for the amination form.

the ene-ynamides²⁴ appear as useful precursors for many reactions, such as the mediated Pauson–Khand reaction²⁵ and cyclotrimerizations,²⁶ en-ynamide ring-closing metathesis by using the second-generation Grubbs’ catalyst,²⁷ Suzuki couplings,²⁸ Eschenmoser–Ficini–Claisen rearrangements,²⁹ cross-couplings,³⁰ or pericyclic reactions.³¹

In a previous work, we have analyzed the formation of 3-azabicyclo[4.1.0]hept-4-enes from 1,6-enynes tethered by heteroatom.^{10b} This study concluded that the reaction mechanism proceeds through an endo-cyclization step followed by a [1,2]-hydrogen shift. The final step is proposed to be assisted by the heteroatom. For eneynamide substrates, it seems evident that the presence of the nitrogen atom attached to the acetylenic unit may control the evolution of the cycloisomerization.

Recent experimental results by Marion et al. have revealed that the catalyzed process leads to the formation of metathesis products (**K**) or bicyclic adducts (**L**), depending on the tether length (Scheme 3).³² Following the cationic manifold proposal by Fürstner, they suggested a formal [2 + 2]-cycloaddition and the intermediacy of bicyclic species **I** on the reaction path. However, the electron-withdrawal nature of the NTs moiety would destabilize such structure. On the basis of the mechanism presumed for metathesis rearrangement,^{9a} the formation

(24) (a) Mulder, J. A.; Kurtz, K. C. M.; Hsung, R. P. *Synlett* **2003**, 1379–1390. (b) Zifcsak, C. A.; Mulder, J. A.; Hsung, R. P.; Rameshkumar, C.; Wei, L.-L. *Tetrahedron* **2001**, *57*, 7575–7606.

(25) (a) Schottelius, M. J.; Chen, P. *Helv. Chim. Acta* **1998**, *81*, 2341–2347. (b) Rainier, J. D.; Imbriglio, J. E. *J. Org. Chem.* **2000**, *65*, 7272–7276. (c) Witulski, B.; Stengel, T. *Angew. Chem., Int. Ed.* **1998**, *37*, 489–492. (d) Witulski, B.; Gössmann, M. *Synlett* **2000**, 1793–1797.

(26) (a) Witulski, B.; Stengel, T. *Angew. Chem., Int. Ed.* **1999**, *38*, 2426–2430. (b) Witulski, B.; Stengel, T.; Fernández-Hernández, J. M. *Chem. Commun.* **2000**, 1965–1966. (c) Witulski, B.; Alayrac, C. *Angew. Chem., Int. Ed.* **2002**, *41*, 3281–3284.

(27) (a) Saito, N.; Sato, Y.; Mori, M. *Org. Lett.* **2002**, *4*, 803–805. (b) Huang, J.; Xiong, H.; Hsung, R.; Rameshkumar, C.; Mulder, J. A.; Grebe T. P. *Org. Lett.* **2002**, *4*, 2417–2420.

(28) Witulski, B.; Buschmann, N.; Bergsträsser, U. *Tetrahedron* **2000**, *56*, 8473–8480.

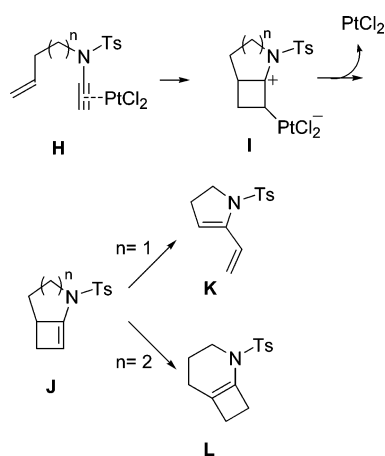
(29) Mulder, J. A.; Hsung, R. P.; Frederick, M. O.; Tracey, M. R.; Zifcsak, C. A. *Org. Lett.* **2002**, *4*, 1383–1386.

(30) (a) Minière, S.; Cintrat, J.-C. *J. Org. Chem.* **2001**, *66*, 7385–7388. (b) Timbert, J.-C.; Cintrat, J.-C. *Chem. Eur. J.* **2002**, *8*, 1637–1640.

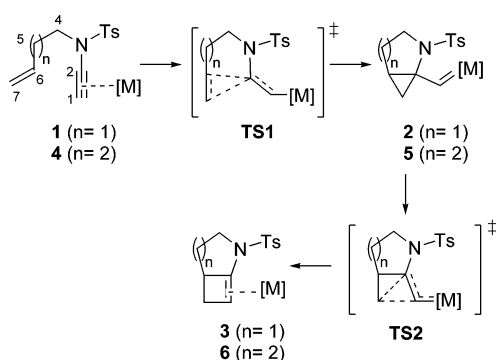
(31) Hsung, R. P.; Zifcsak, C.; Wei, L.-L.; Douglas, C. J.; Xiong, H.; Mulder, J. *Org. Lett.* **1999**, *1*, 1237–1240

(32) Marion, F.; Coulomb, J.; Courillon, C.; Fensterbank, L.; Malacria, M. *Org. Lett.* **2004**, *6*, 1509–1511.

SCHEME 3



SCHEME 4



of the metathesis product ($n = 1$) and the cyclobutene adducts (for longer chains, $n = 2, 3$) suggests a common reaction pathway, whose evolution would be controlled by strain in the cyclobutene **J**. The participation of the cyclobutene in the metathesis is supported by isolation of bicyclo[4.2.0]oct-1(8)-ene structures from 1,7-enynes³³ and isomerized cyclobutenes from 1,6-enynes.^{34,35}

Hence, we propose the reaction mechanism depicted in Scheme 4. The initial complexation of the alkyne onto the electrophilic catalyst triggers the intramolecular nucleophilic attack of the alkene, through an exo-cyclization. In contrast with the alkyl precursor, the presence of a bulky electron-withdrawal moiety induces the formation of a slipped η^1 -complex rather than a η^2 -complex (Pt–C₁ = 1.936, Pt–C₂ = 2.772 Å; see Figure 1), **1**. This enhances the electrophilic activation of the internal acetylenic carbon and promotes an exo-cyclization, inhibiting the endo-route, as NPA charges suggest (C₁ = –0.324 vs C₂ = +0.325). The internal carbon of the activated alkyne reacts with the nucleophilic C₆=C₇ bond through a later transition structure **TS1** (C₂–C₆ = 2.313 Å; C₂–C₇ = 2.183 Å) than that for simple 1,6-enynes.^{9a} The formation of the cyclopropylmetallacarbene **2** is exothermic (–7.15 kcal mol^{–1}, Table 1) and proceeds with an activation energy of 11.39 kcal mol^{–1}, a less favorable results than those for the simple enyne pattern due to the effect of

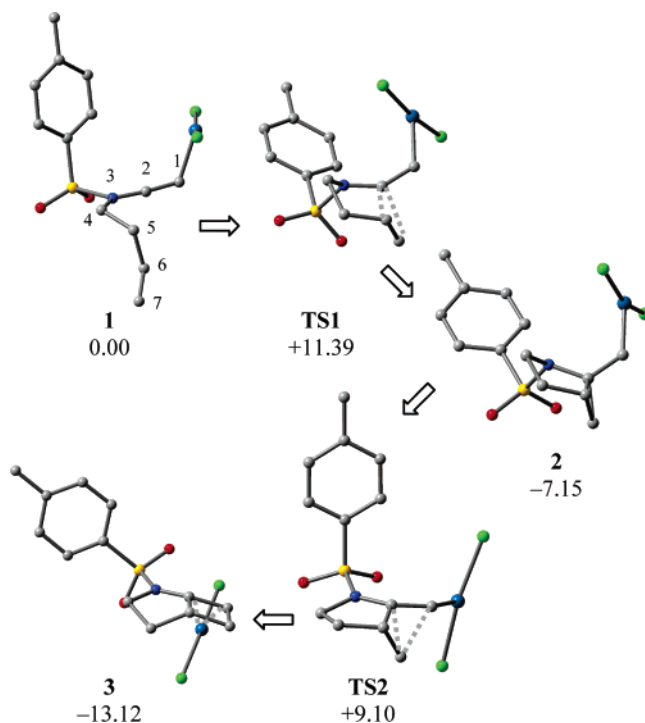


FIGURE 1. Optimized structures for the PtCl₂-mediated formation of **3**. Relative free energies are given in kcal mol^{–1} (H atoms have been omitted for clarity).

the heteroatom. Indeed, the C–N bonds are shorter than the C–C bonds, which implies a higher annular tension.

The subsequent rearrangement of the fused cycle through the attack of the carbene carbon takes place via **TS2**, which clearly shows the cleavage of the cyclopropane ring (C₂–C₇ = 1.790 Å) and the incipient formation of the cyclobutene framework (C₁–C₇ = 2.112 Å). IRC calculations confirm that this transition state structure evolves to the expected π -coordinated cyclobutene intermediate **3**. This step is exothermic (–5.97 kcal mol^{–1}, **3** being –13.12 kcal mol^{–1} below the reactant complex) and proceeds with a moderately low activation energy (16.25 kcal mol^{–1}), as compared with the enyne model, because the heteroatom stabilizes the N–C₂–C₁–Pt fragment by an effective π -delocalization in **TS2** (N–C₂–C₁–Pt dihedral angle = 5.8°).

Table 1 summarizes the calculated total and free energy values for 1,6- and 1,7-ene-ynamides. As expected, the exo cyclization for a longer 1,7-enyne (**4**) is more exothermic than for the 1,6-precursor. The metallacyclopropylcarbene intermediate leads to the π -coordinated bicyclo[4.2.0]octene **5** with a slightly higher energy barrier than the formation of the bicyclo[3.2.0]heptene counterpart. Nevertheless, the less strained six-membered ring **6** predictably gives rise to lower energy values relative to the reactant complex, as compared with the five-membered heterocycle. The introduction of a *gem*-dimethyl group on the tether induces a reduction of the activation energy for the exo-cyclopropanation step. This effect, known as the *gem*-dialkyl effect, agrees with the experimental observations. As indicated by our results, it can be attributed to the “reactive rotamer effect”,³⁶ and not to angle compression³⁷ (“Thorpe–Ingold effect”).

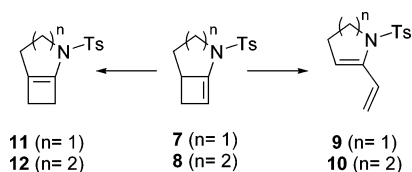
The isomerization of the double bond from the bridgehead position further stabilizes the bicyclic framework

(33) Trost, B. M.; Yanai, M.; Hoogsteen, K. *J. Am. Chem. Soc.* **1993**, *115*, 5294–5295.

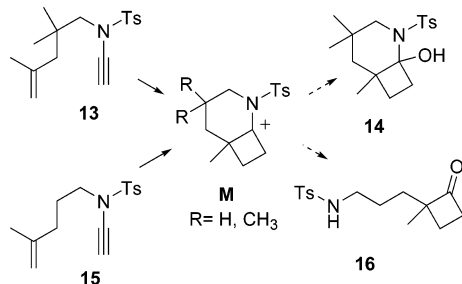
(34) Trost, B. M.; Trost, M. K. *J. Am. Chem. Soc.* **1991**, *113*, 1850–1852.

(35) Fürstner, A.; Davies, P. W.; Gress, T. *J. Am. Chem. Soc.* **2005**, *127*, 8244–8245.

SCHEME 5



SCHEME 6



for the 1,7-derivative (Table 2). At this point, the energy differences between both tether length models are noteworthy and support a divergent evolution. While the isomerization from the uncomplexed cyclobutene **8** to **12** is thermodynamically favored, the process seems less likely for the fused 4–5 ring system, given the lower stability for the isomerized adduct **11** as compared with **7**. Instead, the severe ring strain promotes the (conrotatory) electrocyclic ring opening of the cyclobutene **7**, through the transition structure **TS3** ($C_6-C_7 = 2.127 \text{ \AA}$), to afford the highly stable conjugated diene **9** (Scheme 5, Table 2). This process is less favored for the less tensioned bicyclo[4.2.0]octene framework from both kinetic and thermodynamic points of view, even when bearing a *gem*-dimethyl substitution on the tether.

On the other hand, the lability of the bicyclic skeleton may lead to further transformations under the proper conditions. Thus, the hydrolysis of these intermediates under acidic conditions drives to cyclobutanones and/or bicyclic aminals.³² The poly-substituted precursor **13** furnishes the bicyclic aminal **14**, whereas a less substituted enyne, such as **15**, affords the cyclic ketone **16** (Scheme 6). Since the authors did not provided stereochemistry assignation for **14** nor a rationalization to account for its formation,³² we cautiously present additional insights on the basis of electronic, steric, and energetic details.

Taking into account the expected hydrolysis mechanism under acidic conditions, the initial protonation may yield two possible carbocations **M** due to the presence of the methyl group at the ring junction, so the subsequent nucleophilic addition can generate four stereoisomers. The computed LUMO maps on the carbocations clearly indicate that the syn-nucleophilic attack would be favored over the anti-attack (see Supporting Information). In addition, the lower ring strain for a *cis*-fused cyclobutane expectedly drives the *cis* isomers to a higher stability in any case. On the other hand, the simultaneous substitution on the alkene and the tether induces a strong destabilizing 1,3-interaction of the *gem*-dimethyl moiety

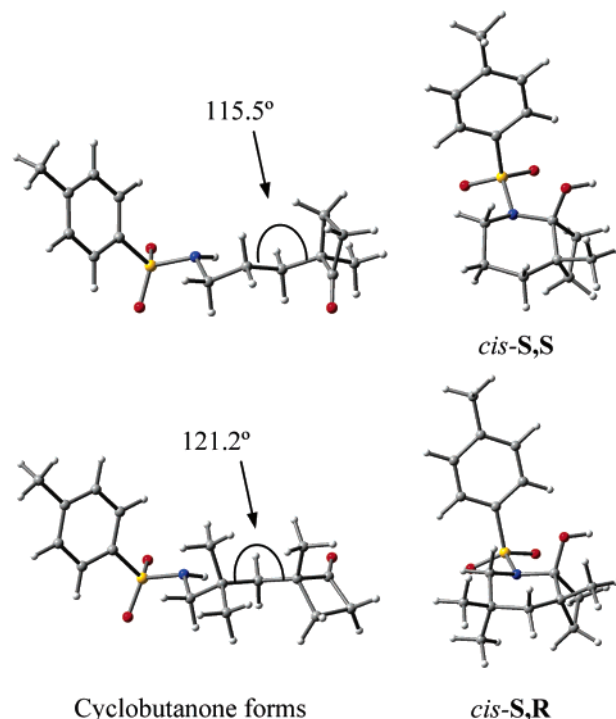


FIGURE 2. Optimized geometries for aminal and cyclobutanone forms. The destabilizing 1,3-interaction for the *gem*-dimethylcyclobutanone derivative forces the opening of the marked bond angle (left bottom) as compared with the unsubstituted cyclobutanone (left top).

and the substituted cyclobutanone (Figure 2), which precludes its formation, favoring the bicyclic aminal (Table 3). On the contrary, the lack of this interaction leads to the most stable cyclobutanone form, in total agreement with the experimental observations.

2. PtCl₂-Mediated Cycloisomerization of En-1-yn-3-ol Systems. Continuing with the study of these highly substrate-dependent processes, we next discuss the effect of the substitution on the tether as well as the tether length for precursors functionalized at the propargylic site.

As has been mentioned above, tertiary^{8,38} and secondary³⁹ propargylic acetates have been found to yield cyclic enolesters derivatives⁴⁰ upon treatment of 1,6-enynes with electrophilic transition-metal complexes, such as Pt(II) and Pd(II) complexes. Such products are synthetically important as efficient precursors of cyclic-ketones building blocks. This process has been successfully performed with different transition-metal complexes on 1,6-,⁴¹ 1,5-^{39,42,43} and 1,4-enynes.⁴⁴

However, from a mechanistic point of view, a controversy about the true reaction pathway still remains. Thus, while many authors have systematically assumed a [1,2]-acyl migration followed by a cyclization step as the mechanistic pathway, our previous theoretical results

(38) Anjum, S.; Marco-Contelles, J. *Tetrahedron* **2005**, *61*, 4793–4803.

(39) Harrak, Y.; Blaszykowski, C.; Bernard, M.; Cariou, K.; Mainetti, E.; Mouries, V.; Dhimane, A.-L.; Fensterbank, L.; Malacria, M. *J. Am. Chem. Soc.* **2004**, *126*, 8656–8657.

(40) For a pioneering Pd(II)-catalyzed cycloisomerization, see: Rautenstrauch, V. *J. Org. Chem.* **1984**, *49*, 950–952.

(41) For the AuCl₃-catalyzed cycloisomerization, see: Fürstner, A.; Hannen, P. *Chem. Commun.* **2004**, 2546–2547.

(36) (a) Jung, M. E.; Gervay, J. *J. Am. Chem. Soc.* **1991**, *113*, 224–232. (b) Lightstone, F. C.; Bruice, T. C. *J. Am. Chem. Soc.* **1994**, *116*, 10789–10790.

(37) Further details are provided as Supporting Information.

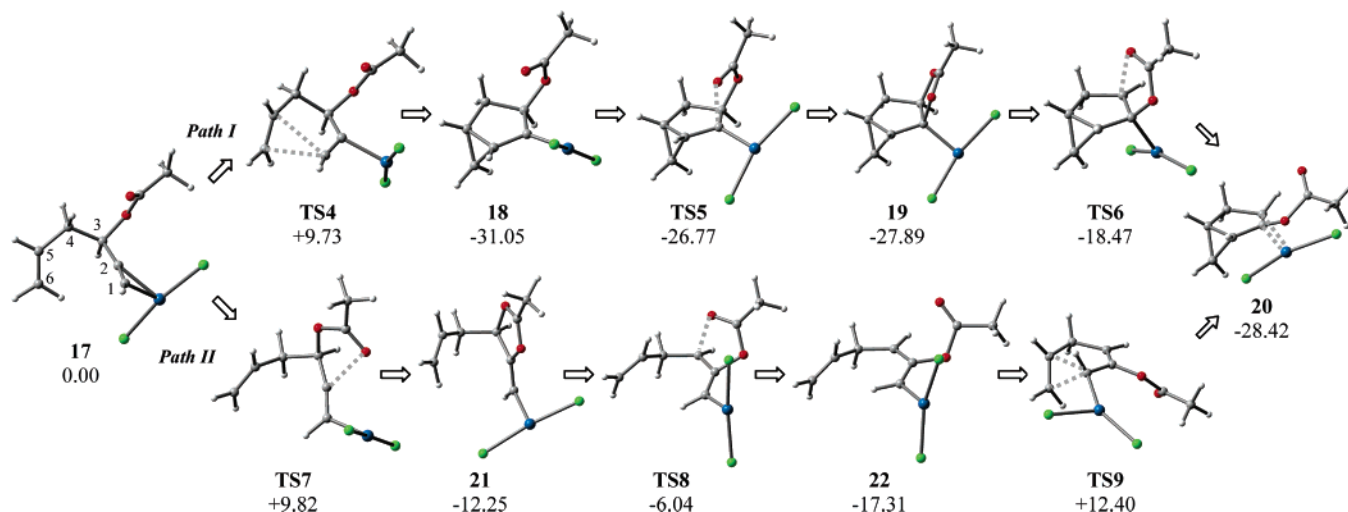
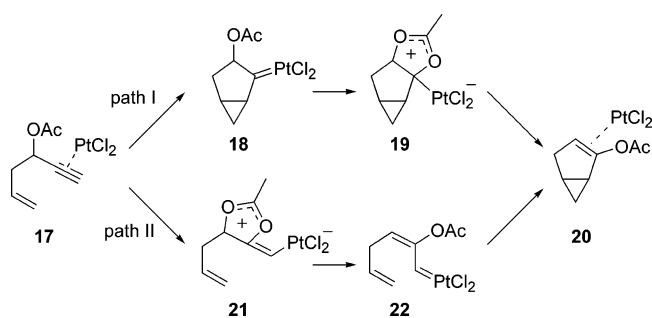


FIGURE 3. Optimized structures for the PtCl_2 -mediated formation of **20** through two different reaction pathways (see Scheme 7). Relative free energies to the reactant complex are given in kcal mol^{-1} .

SCHEME 7



for 1,6-enyne substrates have suggested an inverse sequence, i.e., cyclopropanation and then [1,2]-migration, as a more favored route from kinetic and thermodynamical viewpoints.

Since the cyclization as the first step for short 1,5-enynes may be more problematic, therefore supporting an initial [1,2]-acyl migration for the cycloisomerization process, we now have reexamined both plausible mechanisms. So, we have analyzed the transformation of the precursor **17** into the bicyclic enol ester **20** and initially we have considered path I (Scheme 7). The η^2 -complex⁹ **17** formed by coordination of the alkyne to the metal complex affords the platinacarbene **18** through an endo-cyclization step. The involved transition structure **TS4** is more asymmetric ($C_1-C_5 = 2.549$, $C_1-C_6 = 2.430$ Å) than that for the 1,6-enyne analogues ($C_1-C_6 = 2.498$, $C_1-C_7 = 2.491$ Å). As expected, this step proceeds with a higher activation energy (9.73 vs 7.02 kcal mol^{-1} for 1,6-enyne patterns) and is less exothermic (-31.05 vs -33.40 kcal mol^{-1}).

Then, the [1,2]-acyl migration takes place through a stepwise process that is initiated by an initial intramolecular nucleophilic attack of the carbonyl oxygen atom

on the electrophilic carbene.⁴⁵ This stepwise process involves two low-energy barriers (4.29 and 9.42 kcal mol^{-1}), which predictably are similar to our previous results for 1,6-enyne,^{9b} since such migration would be unaffected by the ring size. The overall reaction is somewhat less exothermic (-28.42 vs -30.75 kcal mol^{-1}), due to the higher tension of the bicyclo[3.1.0]hexene framework. The optimized structures are shown in Figure 3.

On the contrary, the electrophilic activation of the alkyne by the metal complex may also trigger an anchimerically assisted 1,2-addition of the ester to generate the vinyl carbene intermediate **22** (path II). Calculations reveal that this stepwise process proceeds initially through **TS7**, with an activation energy analogous to that computed for a 1,6-enyne system (9.82 vs 9.51 kcal mol^{-1}), to yield the heterocycle **21**. This first step is considerably less exothermic than the first step for path I (-12.25 vs -31.05 kcal mol^{-1}). Then **21** evolves through **TS8**, involving a low-energy barrier (6.21 kcal mol^{-1}), to afford the vinyl platinum species **22**. In the light of these results, the real reaction path appears very uncertain. Nevertheless, the cyclization step of trapping of the carbene by the alkene also emerges as acutely affected by a shorter tether chain and takes place with a very high activation energy, 29.71 kcal mol^{-1} , being the transition structure **TS9** + 12.40 kcal mol^{-1} above the reactant complex.

Hence, these results indicate that the tether length has a deeper influence on the intramolecular cyclopropanation step for path II than for path I. This is probably due to a conformational energy penalty. Thus, while the approaching between the reactive centers to reach **TS4** (path I) is aided by a flexible $-\text{CH}_2-\text{CH}_2-$ chain, the vinyl-Pt intermediate **22** (path II) presents one bridge methylene group between two alkene moieties, which makes the proper conformational rearrangement difficult for an effective orbital overlapping to achieve the cyclopropanation transition state.

These observations support our previous mechanistic picture for PtCl_2 -mediated cycloisomerization of 1,6-enynes bearing tertiary propargylic carboxylates. In this context, it has been reported by Harrak et al.³⁹ that the

(42) Błaszykowski, C.; Harrak, Y.; Gonçalves, M. H.; Cloarec, J. M.; Dhimane, A. L.; Fensterbank, L.; Malacria, M. *Org. Lett.* **2004**, *6*, 3771–3774.

(43) Mamane, V.; Gress, T.; Krause, H.; Fürstner, A. *J. Am. Chem. Soc.* **2004**, *126*, 8654–8655.

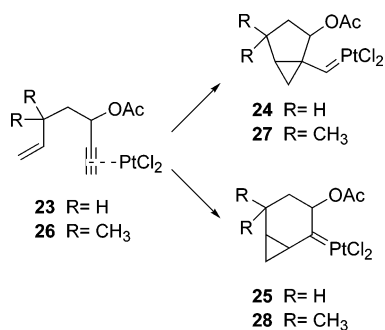
(44) For Au(I)-catalyzed cycloisomerization, see: Shi, X.; Gorin, D. J.; Toste, F. D. *J. Am. Chem. Soc.* **2005**, *127*, 5802–5803.

(45) Herndon, J. W.; Wang, H. *J. Org. Chem.* **1998**, *63*, 4564–4565.

TABLE 4. Effect of the *gem*-Dimethyl Group on the Tether on the Total^a and Free^b Energy Differences for the First Step of the PtCl₂-Mediated Cycloisomerization of 1,6-Enynes with a Propargylic Carboxylate Substituent^c

5-exo path	ΔE (kcal mol ⁻¹)	ΔG_{298} (kcal mol ⁻¹)	6-endo path	ΔE (kcal mol ⁻¹)	ΔG_{298} (kcal mol ⁻¹)
23	0.00	0.00	23	0.00	0.00
TS	4.67	6.55	TS	7.06	8.71
24	-32.79	-29.95	25	-37.38	-34.54
26	0.00	0.00	26	0.00	0.00
TS	3.87	5.10	TS	5.05	6.30
27	-35.25	-33.01	28	-39.24	-35.83

^a Zero-point corrected values. ^b Includes thermal corrections at 298 K. ^c See Scheme 8 for numbering.

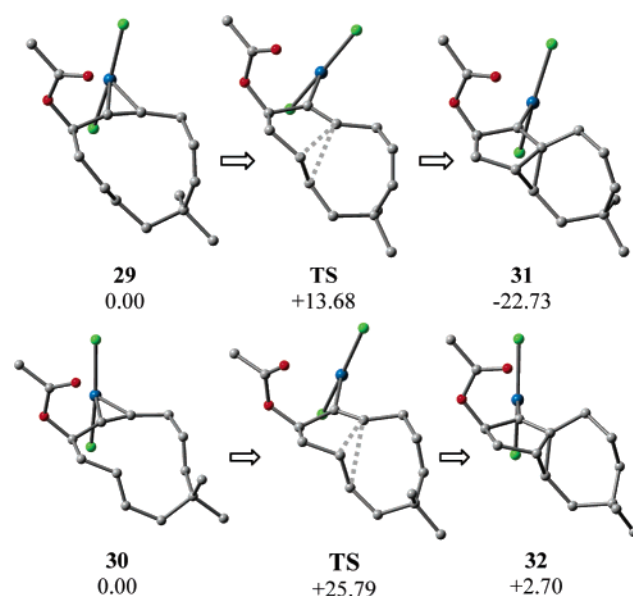
SCHEME 8

cycloisomerization of secondary analogues provides divergent results. So, the Pt(II)-catalyzed transformation of unsubstituted 1,6-enynes affords the metathesis-type product, whereas the introduction of a *gem*-dimethyl group on the tether gives rise to both the metathesis adduct and bicyclic [4.1.0] derivative. This simple comparison confirms the critical steric role of the substituents on the metathesis rearrangement.^{9a}

For 1,6-enyne systems, it was found from DFT calculations that an initial 5-exo cyclization step is faster than a 6-endo route to form a platinum-carbene (Scheme 1).^{9a} Since the metathesis rearrangement for simple 1,6-enyne systems has been proposed to proceed via 5-exo cyclopropanation, it appears as the favored route. In contrast, the *gem*-dimethyl group may induce a different magnitude of the presumed effects on each path: a favorable “*gem*-dialkyl effect”, and an unfavorable steric hindrance.

To gain insights into this subject, further calculations were performed and the results are summarized in Table 4 (see Scheme 8). Although the 5-exo cyclization is kinetically favored over the endo-path in any case, the introduction of the *gem*-dimethyl substitution on the tether induces a greater effect on the later route. Accordingly, while the energy difference between both transition states for the unsubstituted precursor is >2 kcal mol⁻¹, it reduces to about 1 kcal mol⁻¹ by introducing such substitution. That is, the “*gem*-dialkyl effect” induces an upper acceleration for the 6-endo cyclization.

In view of the synthetic potential and in order to extend the scope of the method, these transition-metal-catalyzed reactions have also been applied to macrocyclic enynes.⁴² In that case, the access to tricyclic systems with an inner cyclopropane ring appears as a highly stereocontrolled reaction due to ring restrictions. Regarding this question, an additional unsaturation on the macrocycle has been found to play a critical role in the transannular cyclo-

**FIGURE 4.** Optimized structures for the first step of the PtCl₂-mediated cycloisomerization of *Z,E*- (top) and *E,E*-macrocyclic enynes (bottom). Relative free energies are given in kcal mol⁻¹ (H atoms have been omitted for clarity).

somerization outcomes. Thus, while the *Z,E*-cycloundecadienyne **29** generates diastereoselectively the predictable tricyclic ketone, the *E,E*-counterpart **30** provides the allene³⁸ in low yield. On the basis of the reaction mechanism suggested by DFT calculations, the cyclopropanation (first) step has been found to be kinetically accessible, under the employed conditions, only in the former case. So, the activation energy for the *Z,E*-precursors (**29**) is 13.68 kcal mol⁻¹, about 4 kcal mol⁻¹ higher than for the acyclic 1,5-enyne, and the formation of the cyclopropylplatinacarbene **31** is about 8 kcal mol⁻¹ less exothermic due to the expected restricted freedom (Figure 4). However, the introduction of a *trans*-alkene moiety on such macrocycle (**30**) results in a high activation energy, 25.79 kcal mol⁻¹, and, more strikingly, an endothermic cyclopropanation step (2.70 kcal mol⁻¹). Hence, this process is strongly disfavored from both kinetic and thermodynamical viewpoints. Instead, the formation of the allene **33** from the *E,E*-precursor proceeds through a more favorable energy profile. Following the stepwise [1,3]-acyl migration mechanism proposed elsewhere,^{9b} the computed values (Figure 5) reveal that the first step takes place with a moderately low activation energy (10.61 kcal mol⁻¹) and is exothermic by -10.62 kcal mol⁻¹, while the second step involves an energy barrier of 7.44 kcal mol⁻¹, being slightly endothermic (3.96 kcal mol⁻¹). These results are parallel to those computed for a 1,6-enyne acyclic system, although thermodynamically less favorable since the overall reaction is rather less exothermic (-6.66 kcal mol⁻¹).

As expected, the computed atomic charges for the activated cyclic alkyne (reactant complex) are different from those calculated for acyclic 1,5- or 1,6-enynes (+0.010 - +0.035 for the internal and -0.185 for the terminal alkyne carbon). Thus, the *Z,E*-isomer shows -0.014 and +0.073 values and the *E,E*-isomer -0.003 and +0.052 for analogous positions, respectively. These results indicate a higher electrophilic activation of the second position due to the alkyl substituent, which may

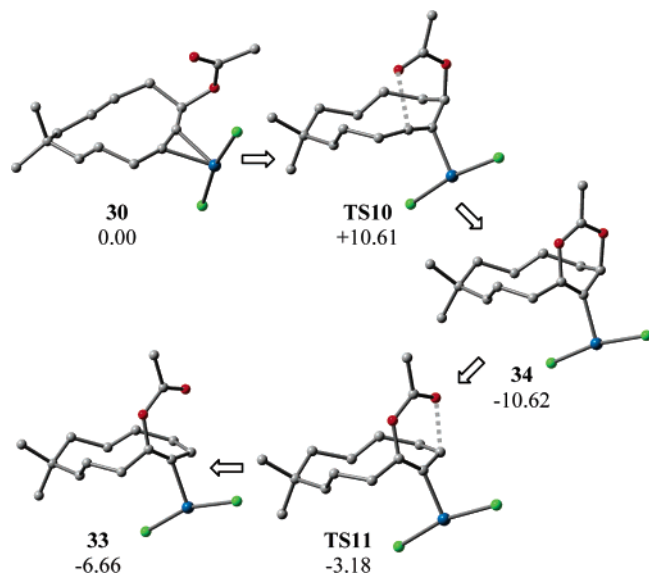


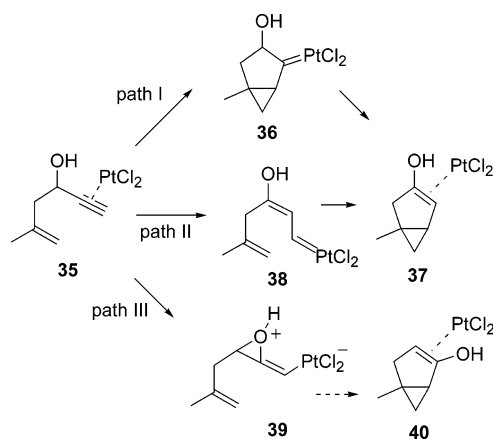
FIGURE 5. Optimized structures for the PtCl_2 -mediated formation of allene **33** from the E,E -macrocylic enyne **31** (free energy differences relative to reactant complex are given in kcal mol^{-1}).

imply two consequences: (i) for substituted alkynes, the endo-cyclopropanation should be favored over the exo-route, not only by the relieved ring strain effects but also by electronic factors, in contrast with unsubstituted alkyne precursors; (ii) if the alternative proposal path II were the operative mechanism, then the initial [1,2]-acyl migration step should be less favored. To test this hypothesis, we performed further calculations that reveal that this step shows a rather high activation energy ($22.07 \text{ kcal mol}^{-1}$ for the Z,E -isomer, and $22.14 \text{ kcal mol}^{-1}$ for the E,E -isomer). Amazingly, these findings support path I as active mechanism versus path II and, likewise, confirm the mechanistic picture proposed by us for the formation of the allene adduct through a simple [1,3]-acyl migration, in opposition to the reaction pathway suggested by Blaszykowski et al. through two consecutive migration processes.⁴²

This mechanistic scheme through a cyclopropanation step followed by a [1,2]-migration is not restricted to propargylic carboxylates. In fact, DFT calculations have previously revealed that the kinetically preferred pathway for the Pt(II) -mediated cycloisomerization of heteroatom-tethered enynes also involves a [1,2]-hydrogen shift as the second step after an endo-cyclization step.^{10b} Hence, a common mechanistic picture for substrates functionalized at the propargylic site can be deduced, with groups showing contrasting migration abilities. In the former case, the migration is allowed by the anchimeric capacity of the carboxylate moiety, while in the latter it may be assisted by the fixed heteroatom on the tether.

In this context, some authors have postulated that a nonparticipating heteroatom at the nontethered propargylic position, such as a hydroxy or ether group, may promote an initial [1,2]-H migration to the activated alkyne carbon.³⁹ For terminal alkynes, it has been found that the acetylenic bond is polarized in the π -complexed reactant complex, the internal carbon being more electrophilic than the external center. Therefore, if that assumption were correct, it could be deduced that the

SCHEME 9



more nucleophilic OX group should move faster to the electrophilic site rather than a H atom.

To check this hypothesis, we have analyzed the free hydroxy precursor **35** evolving through the expected pathway on the basis of our previous theoretical results (path I, Scheme 9), through an initial [1,2]-H shift (path II, Scheme 9) and via [1,2]-hydroxy migration (path III, Scheme 9). The computed results are depicted in Figure 6 and clearly show that path I, through initial endo-cyclopropanation to form **36**, is the kinetically favored route (activation energy of 7.41 vs 14.39 and $13.13 \text{ kcal mol}^{-1}$ for path II and III, respectively), consistent with the reported data for the formation of bicyclic derivatives from heteroatom-tethered enynes.^{10b} These results correctly account for the formation of **37** versus the alternative regioisomeric product **40** on the basis of kinetic and thermodynamic reasons and support the proposed reaction pathway.

Finally, we focus on one amazing example showing that the efficacy of these stereospecific reactions may be dependent on the stereochemistry of the precursor double bond for acyclic derivatives as well. The Pt(II) -mediated cycloisomerization of the styryl derivative provides higher yields for the E -(**41**) than for the Z -precursor (**42**).³⁹ Optimized geometries (Figure 7) have shown that the phenyl substituent is coplanar in the transition structure with the double bond for the E -isomer, thus enhancing its nucleophilicity by an effective electron donation by the resonance effect. On the contrary, the steric repulsion between the aromatic H and the allylic positions prevents the coplanarity, which results in a destabilization of the Z -derivative transition state structure.⁴⁶ Consequently, the cyclopropanation step proceeds with a high activation energy for the Z -isomer (Figure 7).

To sum up, the results described throughout this paper not only account for these specific experimental observations but also provide further support for the unified mechanistic scheme for the skeletal rearrangement and the formation of fused cyclopropane frameworks from enynes, upon treatment with electrophilic metal complexes.

(46) NBO analysis clearly reveals a hyperconjugation effect between the π -phenyl system and the antibonding orbital of the alkene moiety $\pi^*_{\text{C5-C6}}$ (interaction $\pi_{\text{CPh-CPh}} \rightarrow \pi^*_{\text{C5-C6}}$), which results in a hyperconjugation stabilizing energy of 14.45 for the Z - vs $16.83 \text{ kcal mol}^{-1}$ for the E -derivative transition state structure, supporting the observed trend.

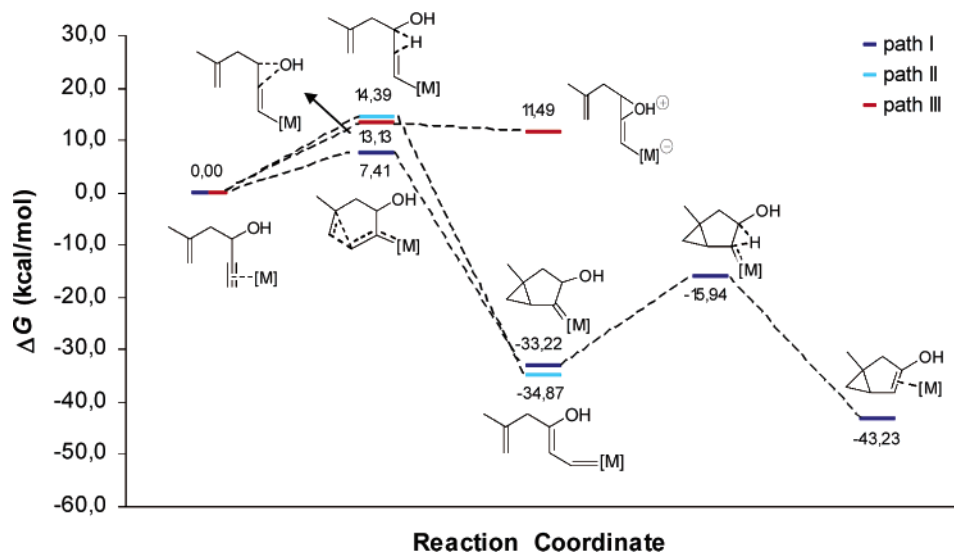


FIGURE 6. Free energy profiles for the PtCl₂-catalyzed cycloisomerization of **35** according to the paths proposed in the Scheme 9 (free energy differences relative to reactant complex are given in kcal mol⁻¹).

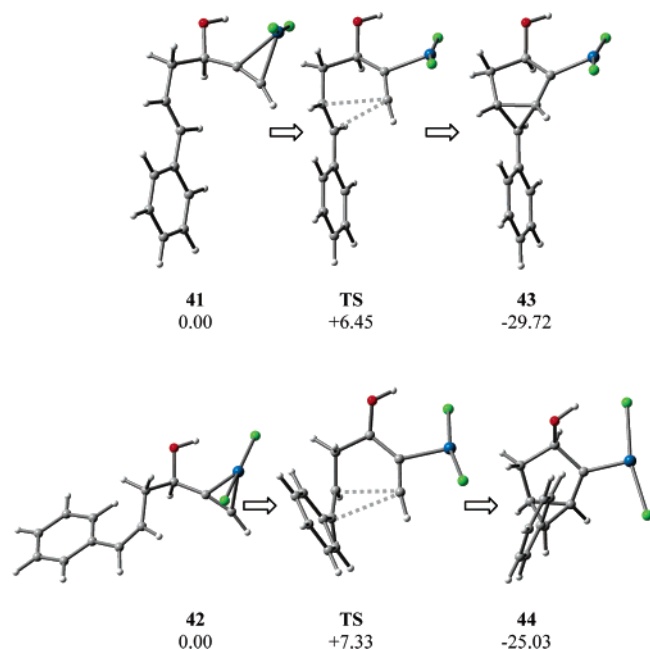


FIGURE 7. Optimized Structures for the first step of the PtCl₂-Mediated Cycloisomerization of *E*- (top) and *Z*- (bottom) styryl derivative. Relative free energies are given in kcal mol⁻¹.

Conclusions

The electrophilic activation of enyne substrates by coordination to electrophilic transition-metal complexes is an outstanding phenomenon that may afford a wide range of cyclic products, depending on the molecular structure. Moreover, most of these intramolecular transformations take place under regio- and stereochemical control, which makes them attractive in the synthesis of optically active cyclic compounds. Despite the high versatility, many of these processes could be closely related from a mechanistic point of view. On the basis of theoretical calculations, we have proposed a unified

mechanistic picture: the activation of the triple bond by a metal center generates electrophilic species and triggers the intramolecular nucleophilic attack of the double bond by an endo- or exo-pathway. Given that both paths are highly substrate-dependent, the formation of one of the possible key metal-cyclopropyl intermediates may be favored, promoting skeleton rearrangements and/or the formation of cyclopropyl-fused rings. The cyclopropyl intermediate formed by exo-cyclopropanation may evolve through divergent routes to yield the metathesis adduct and bicyclic compounds. On the contrary, the endo-cyclization may be followed by a [1,2]-migration of the propargylic moiety to the internal acetylenic position to afford bicyclic [*n*.1.0] derivatives, for hetero-functionalized precursors at the propargylic site. This reaction mechanism should be common even for such different groups as H or carboxylate substituents.

We have also analyzed throughout this paper the effect induced by different structural motifs, such as the role played by a heteroatom directly attached to the triple bond, the tether length, the substitution on the acetylenic position, and the *gem*-dialkyl substitution on the tether. The theoretical results obtained can rationalize and account for the experimental observations accumulated in the last years on this emergent field and, amazingly, support the proposed reaction paths based on that common mechanistic scheme.

Acknowledgment. We thank Prof. Max Malacria (UPMC, Paris, France) and Prof. Paloma Ballesteros (UNED, Spain) for continuous support and encouragement. E.S. thanks Gobierno de La Rioja for a postdoctoral fellowship.

Supporting Information Available: LUMO maps computed on the carbocations **M**, analysis of the “*gem*-dialkyl effect”, a comparison between B3LYP and MP2 methods, and atomic coordinates for the computed structures. This material is available free of charge via the Internet at <http://pubs.acs.org>.

JO0514265